Hyperfine Interact (2012) 207:53–59
DOI 10.1007/s10751-011-0421-6

Unfolding the role of iron in Li-ion conversion electrode materials by ^{57}Fe Mössbauer spectroscopy

José L. Tirado · Pedro Lavela · Carlos Pérez Vicente · Bernardo León · Candela Vidal-Abarca

Published online: 28 October 2011

Abstract ^{57}Fe Mössbauer spectroscopy is particularly useful in the study of oxide and oxalate conversion anode materials for Li-ion batteries. After reduction in lithium test cells, all these materials showed Mössbauer spectra ascribable to iron atoms in two different environments with superparamagnetic relaxation. The spectra recorded at 12 K revealed the ferromagnetic character in agreement with particle sizes of ca. 5 nm. The two types of iron can be ascribed then to surface and core atoms. Core iron atoms play an important role to retain high faradic capacity values for a large number of cycles. These atoms are preserved from irreversible reactions with the electrolyte and hence they promote a high reversibility and rate capability.

Keywords Conversion anode materials · Lithium-ion batteries · ^{57}Fe Mössbauer spectroscopy

1 Introduction

The future of electrochemical energy storage devices in transport applications is dependent on the development of higher capacity systems. The future "superbatteries" may be found in new technologies such as lithium-air or lithium-sulfur [1]. However, the lithium-ion related concepts still have serious possibilities of improvement. For the negative electrode, a minimum requirement is doubling the capacity of the conventional graphite electrode, which for example could increase the travel distance of an EV on a single electric charge.

In lithium-ion batteries, lithium metal is replaced by different compounds in order to avoid the problems associated with the poor reconstruction of the surface of the

J. L. Tirado (✉) · P. Lavela · C. Pérez Vicente · B. León · C. Vidal-Abarca
Laboratorio de Química Inorgánica, Universidad de Córdoba, Edificio Marie Curie, Campus de Rabanales, 14071 Córdoba, Spain
e-mail: iq1ticoj@uco.es

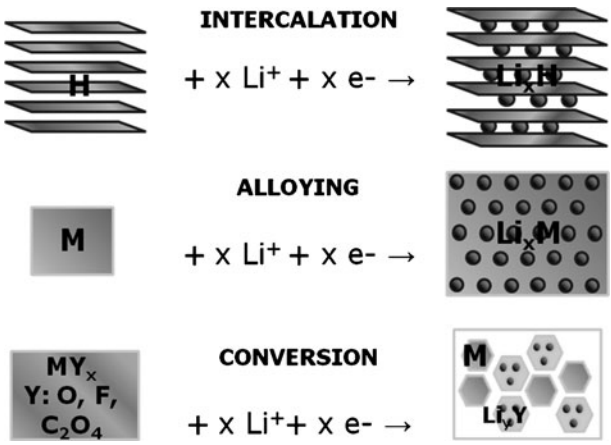

Fig. 1 Types of anode materials for Li-ion battery

lithium electrode on cycling. In general, the complete Li-ion battery can be written as: A/Electrolyte/C, where A and C are the anode and cathode, respectively, provided that C has a higher potential than A vs. Li/Li^+. When studying electrode materials for Li-ion batteries, it is common to use lithium test cells such as Li/Electrolyte/A or Li/Electrolyte/C, in which both A and C act as cathodes vs. lithium. However, they still can be referred to as A, (potential) anode material (for lithium-ion batteries), and C, (potential) cathode material (for lithium-ion batteries). The known active materials having relatively low potential vs. Li/Li^+, and thus being interesting for the anode (A) of Li-ion batteries, have different chemistries (Fig. 1). Among intercalation compounds, graphite and titanium oxides are currently exploited materials in commercial products. However, even for the promising graphene, capacities never double that of graphite on prolonged cycling [2]. Alloying materials such as tin and silicon may show capacities more than twice that of graphite, but the problems associated to the colossal volume changes associated to lithium addition-extraction damage their cycling properties [3]. Finally, vast group of materials that are known to participate in reversible conversion reactions with lithium were more recently studied [4].

Initially, the unexpected reversibility of the conversion process was reported for binary first-row transition metal oxides, while subsequently it was extended to mixed oxides [5–12]. More recently, we were able to extend the reversible conversion to transition metal oxysalts, such as oxalates and carbonates, in which new mechanisms of charge storage such as double layer capacitive effects were detected [13–17]. Other researchers have extended this group of compounds to metal formates [18].

^{57}Fe Mössbauer spectroscopy is a powerful tool to deepen in the mechanism of reaction during cell charge and discharge of both conversion oxides and oxysalts containing iron. The possibilities of application that will be discussed below include confirmation of the reduction to metallic state to avoid confusion with side processes such as SEI formation or double-layer charge storage, study of the environment(s) of atoms in the reduced electrode, maximum re-oxidation achievable and changes in particle size-magnetic ordering on cycling, which may unveil the origin of capacity retention-fading.

2 Experimental

Different synthesis procedures can be used to obtain mixed oxides with highly homogeneous composition and controlled particle size. Here, MFe_2O_4 oxides were alternatively prepared by a reverse micelles procedures with Span 80 as a surfactant [19] and by using citrate precursors [20]. The synthesis of dihydrate transition metal oxalates $MC_2O_4{\cdot}2H_2O$ was carried out by the reverse micelles method, using isooctane as the oil phase, and cetyltrimethylammonium bromide surfactant and hexanol co-surfactant [13].The resulting hydrated oxysalts were thermally decomposed at 200°C under vacuum to produce the dehydrated forms MC_2O_4.

The electrochemical tests were carried out in two-electrode Swagelok-type lithium test cells were used. The electrodes were prepared by blending the powdered active material (60%) with carbon black (30%) and poly vinylidene fluoride (10%) dissolved in N-methyl-pyrrolidone. The weight of active material in the electrodes for cycling experiments was about 3 mg, and the electrode was 9 mm in diameter. The slurry was cast onto a Cu foil and vacuum-dried at 120°C. As the negative electrode, a lithium foil was used. The electrolyte was a solution of ethylene carbonate-diethyl carbonate in 1:1 weight proportion, including 1 M $LiPF_6$, supported by a porous glass-paper disk. The cells were assembled/disassembled in an Ar-filled glovebox (H_2O, $O_2 < 1$ ppm). Charge/discharge experiments were interrupted at selected voltages and the electrodes removed without relaxation period for spectroscopic and diffraction examination.

^{57}Fe Mössbauer spectra were recorded in transmission mode by using an EG&G constant acceleration spectrometer and a ^{57}Co (Rh matrix) (10 mCi) γ source. The velocity scale was calibrated from the magnetic sextet of a high-purity iron foil absorber. Experimental data were fitted to Lorentzian lines by using a least-squares-based method. The quality of the fit was controlled by the classical $\chi 2$ test. All isomer shifts are given relative to the centre of the α-Fe spectrum at room temperature. The measurements at low temperatures were carried with a CRYOGENICS cryostat coupled to a CRYO.CON temperature controller.

3 Results and discussion

A typical conversion reaction in oxide materials is:

$$MO_x + 2xLi^+ + 2xe^- \rightarrow Li_2O + M \quad (1)$$

The theoretical capacities for mixed oxides are collected in Table 1. All the values are noticeably above the theoretical capacity of graphite (ca. 372 $mAhg^{-1}$). Several iron-containing oxides such as MFe_2O_4 (M: Co, Ni) and $Co_{3-x}Fe_xO_4$ ($x = 1, 3$) ($0 \leq x \leq 1$) were shown to be potential candidates for the negative electrode of future Li-ion batteries. In both cases, the electrochemical reaction with lithium results in the formation of transition metals in their reduced state, together with lithium oxide. Lithium extraction allows the reoxidation of iron [7, 10, 19, 20].

For polycrystalline $NiFe_2O_4$ and $CoFe_2O_4$ samples, the ^{57}Fe Mössbauer showed a ferrimagnetic character [19, 20]. After reduction in lithium test cells to ca. 0 V vs. Li/Li^+, the electrode material showed Mössbauer spectra ascribable to iron atoms in two different environments (Fig. 2, Table 2). Both types of atoms show

Table 1 Theoretical capacities and references of the experimental study for different mixed-oxide conversion electrodes

Compound	Full-conversion theoretical capacity (mA h g^{-1})	Reference
Ni_5MgMnO_8	857	[5]
$NiCo_2O_4$	891	[6]
$NiFe_2O_4$	915	[7]
$ZnFe_2O_4$	889	[8]
$LiCoO_2$	822	[9]
$CoFe_2O_4$	914	[10]
$CuFe_2O_4$	896	[11]
$MnCo_2O_4$	906	[12]

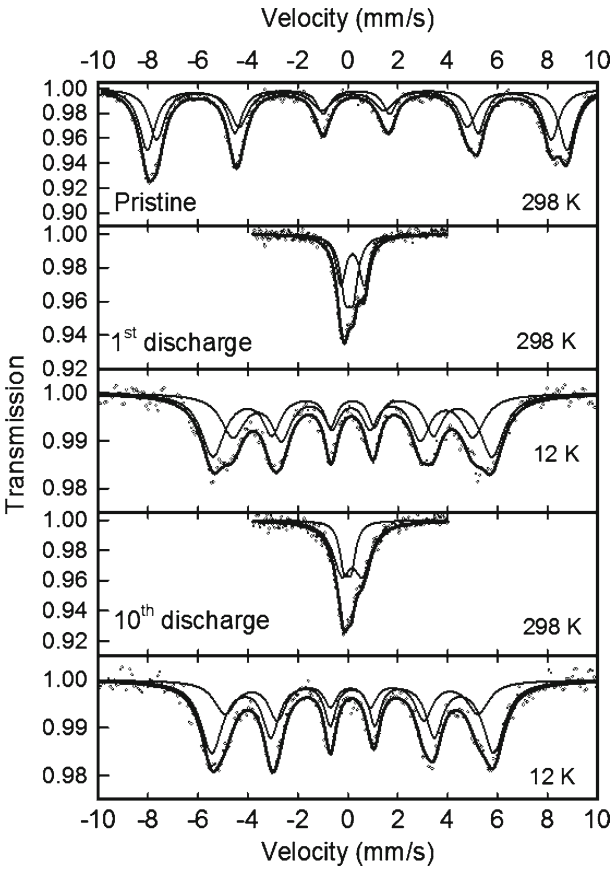

Fig. 2 ^{57}Fe Mössbauer spectra of $NiFe_2O_4$ and discharged electrodes recorded at 298 and 12 K, after 1 and 10 discharges

superparamagnetic relaxation. The spectra recorded at 12 K showed a recovery of the ferromagnetic character (Fig. 2). The reduced blocking temperature implies an enhanced diminution of particle size to ca. 5 nm, in agreement with electron microscopy observations (Fig. 3). The two types of iron can be ascribed then to surface and core atoms. Core iron atoms play an important role to retain high faradic capacity values for a large number of cycles. These atoms are preserved from

Table 2 Hyperfine parameters of pristine and electrochemically reacted electrodes recorded at room temperature

IS isomer shift, *QS* quadrupolar splitting, *LW* line width

Sample	IS	QS	LW	%
FeC_2O_4	1.181_4	1.621_8	0.414_{10}	
reduced	0.00_4	0.68_6	0.5_{10}	37
FeC_2O_4	0.22_3	0.87_3	0.51_4	63
reduced	0.05_1	0.33_1	0.39_3	44
$NiFe_2O_4$	0.17_1	0.92_2	0.51_3	56
reduced	0.04_1	0.00_2	0.61_7	17
$CoFe_2O_4$	0.04_1	0.65_3	0.61_2	83
reoxidized	0.28_2	0.99_3	0.49_6	57
$CoFe_2O_4$	0.25_1	0.49_3	0.49_3	43

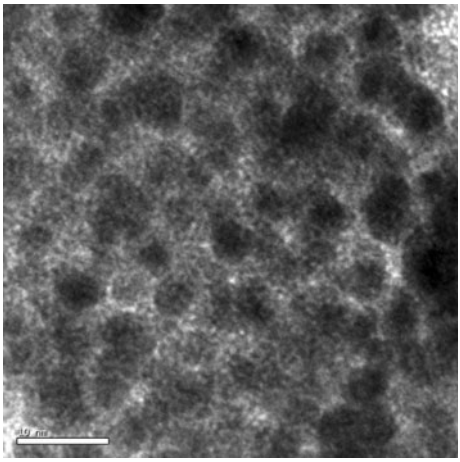

Fig. 3 TEM image of $CoFe_2O_4$ electrode after electrochemical reaction with lithium

irreversible reactions with the electrolyte and hence they promote a high reversibility and rate capability.

After re-oxidation in the cycled electrodes, Fe^{3+} is the main iron contribution, independently from the starting oxidation state of iron in these compounds, which could be interpreted by assuming the existence of Fe^{3+} oxides as well as non-oxidized iron in the solid to compensate for the available anions. Moreover, the two different types of iron atom (core and surface, Table 2) are still observable as quadrupolar doublets indicative of superparamagnetic nanoparticles, although their isomer shift is larger than in the reduced electrodes (Table 2). The size of the particles decreases on further cycling.

A typical conversion reaction of divalent metal oxalates is:

$$MC_2O_4 + 2Li^+ + 2e^- \rightarrow M + Li_2C_2O_4 \quad (2)$$

As compared with transition metal oxides, and irrespective of their different composition, the electrochemical reaction with lithium results in the formation of transition metals in their reduced state, in this case together with lithium oxalate. Lithium extraction allows the reoxidation of iron [13–15].

The RT ^{57}Fe Mössbauer spectra of iron-containing oxalates contain basically a single quadrupole splitted signal (Table 2). The spectrum recorded at 12 K (Fig. 4)

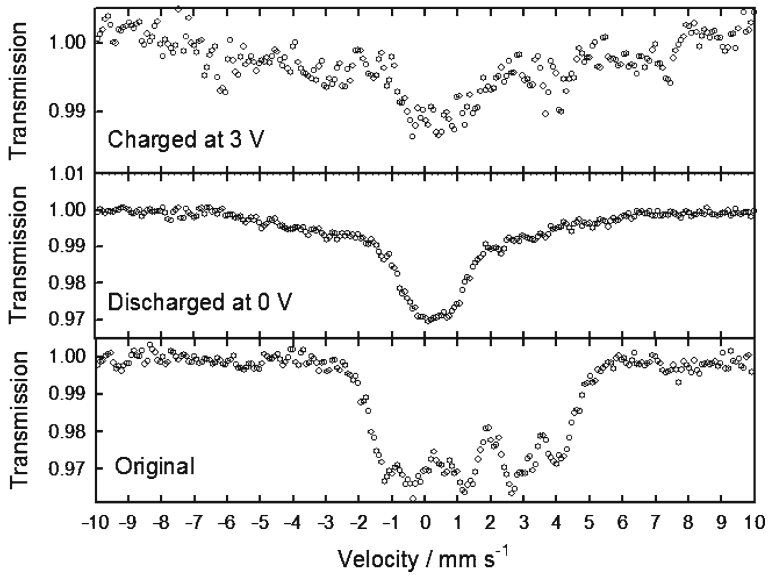

Fig. 4 ^{57}Fe Mössbauer spectra of FeC_2O_4 and used electrodes recorded at 12 K

reveals a poorly resolved cooperative magnetism. The limitations in the recording temperature did not allow discriminating the magnetic components, in agreement with its Néel temperature (11.7 K) [21]. After reduction in lithium test cells to ca. 0 V vs. Li/Li$^+$, the oxalate materials showed Mössbauer spectra ascribable to iron atoms in two different environments [13]. The spectra recorded at 12 K (Fig. 4) does not show the corresponding magnetic sextets. This phenomenon implies a significantly lower lattice coherence length than in the case of oxides. In fact the lower values prevent from direct observation by common electron microscopy techniques. Finally, the recharged electrodes recorded at 12 K reveal the reoxidation to Fe^{3+} with an incipient ferromagnetic component. Summarizing, as compared with oxides, the superparamagnetic state is observable at lower temperatures in the case of iron oxalate. This phenomenon is a consequence of smaller particles, which in turn may condition a significant contribution of the capacitive charge storage mechanism, as recently reported form the $Fe_xCo_{1-x}C_2O_4$ solid solutions [15].

4 Conclusions

Mössbauer spectroscopy has become an irreplaceable tool in the study of different conversion anode materials for Li-ion batteries. Relevant information is obtained on the changes in oxidation state and chemical environment of iron, which are commonly present in various electroactive species. Particularly, the nature of nanocrystalline or amorphous solids involved in the electrochemical reactions, which are reluctant to be characterized by conventional x-ray diffraction methods, can be easily unfolded by Mössbauer spectroscopy. The use of Mössbauer spectroscopy leads to a better understanding of the reaction mechanism, which finally allows an optimized

use of the electrode material. Notorious examples come from the study of nanodispersed materials, which provide large capacities, and improved cyclability.

Acknowledgements The authors are indebted to ERI ALISTORE, MICINN (MAT2008–05880) and Junta de Andalucía (FQM288 and Contract FQM-6017).

References

1. Scrosati, B.: Nature **473**, 448 (2011)
2. Bhardwaj, T., Antic, A., Pavan, B., Barone, V., Fahlman, B.D.: J. Am. Chem. Soc. **132**, 12556 (2010)
3. Besenhard, J.O., Yang, J., Winter, M.: J. Power Sources **68**, 87 (1997)
4. Poizot, P., Laruelle, S., Grugeon, S., Dupont, L., Tarascon, J.M.: Nature **407**, 496 (2000)
5. Alcántara, R., Jaraba, M., Lavela, P., Tirado, J.L.: J. Solid State Chem. **166**, 330 (2002)
6. Alcántara, R., Jaraba, M., Lavela, P., Tirado, J.L.: Chem. Mater. **14**, 2847 (2002)
7. Alcántara, R., Jaraba, M., Lavela, P., Tirado, J.L., Jumas, J.C., Olivier-Fourcade, J.: Electrochem. Commun. **5**, 16 (2003)
8. NuLi, Y.-N., Chu, Y.-Q., Qin, Q.-Z.: J. Electrochem. Soc. **151**, A1077 (2004)
9. Chadwick, A.V., Savin, S.L.P., Alcántara, R., Fernández Lisbona, D., Lavela, P., Ortiz, G.F., Tirado, J.L.: ChemPhysChem. **7**, 1086 (2006)
10. Lavela, P., Tirado, J.L.: J. Power Sources **172**, 379 (2007)
11. Bomio, M., Lavela, P., Tirado, J.L.: ChemPhysChem. **8**, 1999 (2007)
12. Lavela, P., Tirado, J.L., Vidal-Abarca, C.: Electrochim. Acta **52**, 7986 (2007)
13. Aragón, M.J., León, B., Pérez Vicente, C., Tirado, J.L.: Inorg. Chem. **47**, 10366 (2008)
14. Aragón, M.J., León, B., Pérez Vicente, C., Tirado, J.L., Chadwick, A.V., Berko, A., Beh, S.Y.: Chem. Mater. **21**, 1834 (2009)
15. Aragón, M.J., León, B., Serrano, T., Pérez Vicente, C., Tirado, J.L.: J. Mater. Chem. **21**, 10102 (2011)
16. Aragón, M.J., Pérez-Vicente, C., Tirado, J.L.: Electrochem. Commun. **9**, 1744 (2007)
17. Aragón, M.J., León, B., Pérez Vicente, C., Tirado, J.L.: J. Power Sources **196**, 2863 (2011)
18. Saravanan, K., Nagarathinam, M., Balaya, P., Vittal, J.J.: J. Mater. Chem. **20**, 8329 (2010)
19. Vidal-Abarca, C., Lavela, P., Tirado, J. L. : J. Phys. Chem. C, **114**, 12828 (2010)
20. Vidal-Abarca, C., Lavela, P., Tirado, J. L. : Solid State Ionics **181**, 616 (2010)
21. Simizu, S., Chen, J.Y., Friedberg, S.A., Martinez, J., Shirane, G.: J. Appl. Phys. **61**, 3420 (1987)